Sudden Frequency Deviations & Other Phenomena Observed on December 6, 2025

Whitham D. Reeve

An M8.1 x-ray flare erupted at 2029 producing radiation over a very wide frequency range and lasting at least until 2050. The flare immediately altered Earth's dayside ionosphere, producing a Sudden Frequency Deviation (SFD) on the signals received at Anchorage, Alaska from the time-frequency stations WWV in Colorado on 15, 20 and 25 MHz and WWVH in Hawaii on 15 MHz (figure 1). The flare also launched a coronal mass ejection (CME), part of which collided with Earth's magnetosphere a few days later.

Sudden Frequency Deviation

SFD technical concepts are explained in {Reeve15a} and {Reeve15b} but, very briefly, two ionospheric conditions are attributed to sudden frequency deviations, both caused by the x-ray, extreme ultraviolet and ultraviolet energy released by a solar flare. First, a slab of ionosphere below the reflection region undergoes a rapid change in refraction index and, second, the ionosphere's reflection region undergoes a rapid vertical movement. Both conditions introduce a Doppler shift in the radio wave by changing the effective path length (wave number). Either one or both together can cause a sudden frequency deviation.

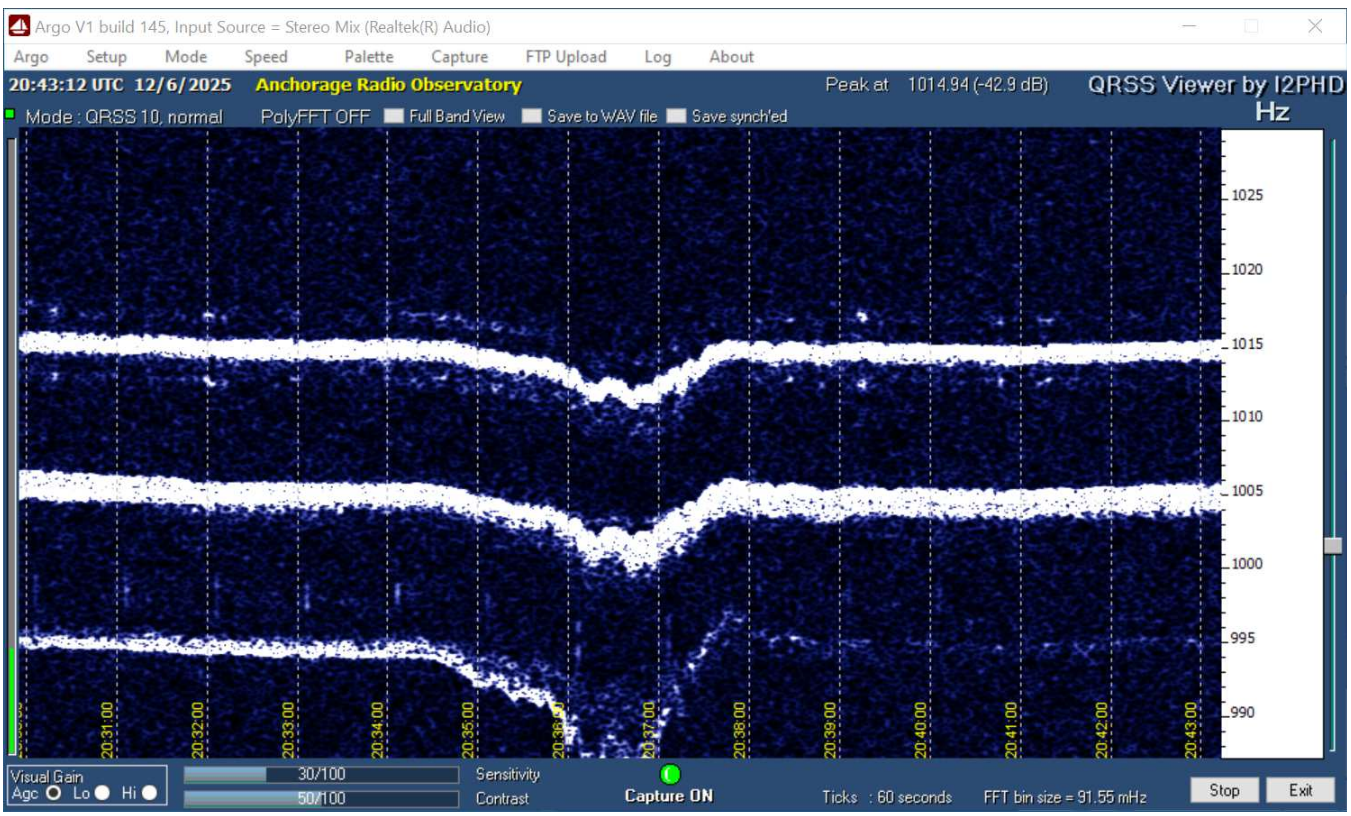

Figure 1 ~ Argo plot above showing the demodulated signals received from WWV and WWVH. The SFD starts about 2034 with estimated 10 Hz deviation at 15 MHz (lower trace) and progressively less deviation at 20 MHz (middle trace) and 25 MHz (upper trace). The 15 MHz trace disappears as a result of the radio blackout from the solar flare radiation increasing the D-region absorption. The higher frequencies did not appear to be as affected. The three receivers were offset tuned by nominal 1 kHz and set to lower sideband (LSB).

Radio Blackout

The SFD was followed by a radio blackout observed at Anchorage on 15 MHz. It is not known if both WWV and WWVH were being received prior to the flare, but WWV on 15 MHz usually is very weak compared to WWVH. The D-RAP plot (figure 2) indicates that the blackout was more likely on the WWVH path. A blackout is caused by excessive ionization and collisions in the D-region that absorb and attenuate the radio waves as they enter the D-region on their way up to a higher refractive region and then are attenuated again on their way back down.

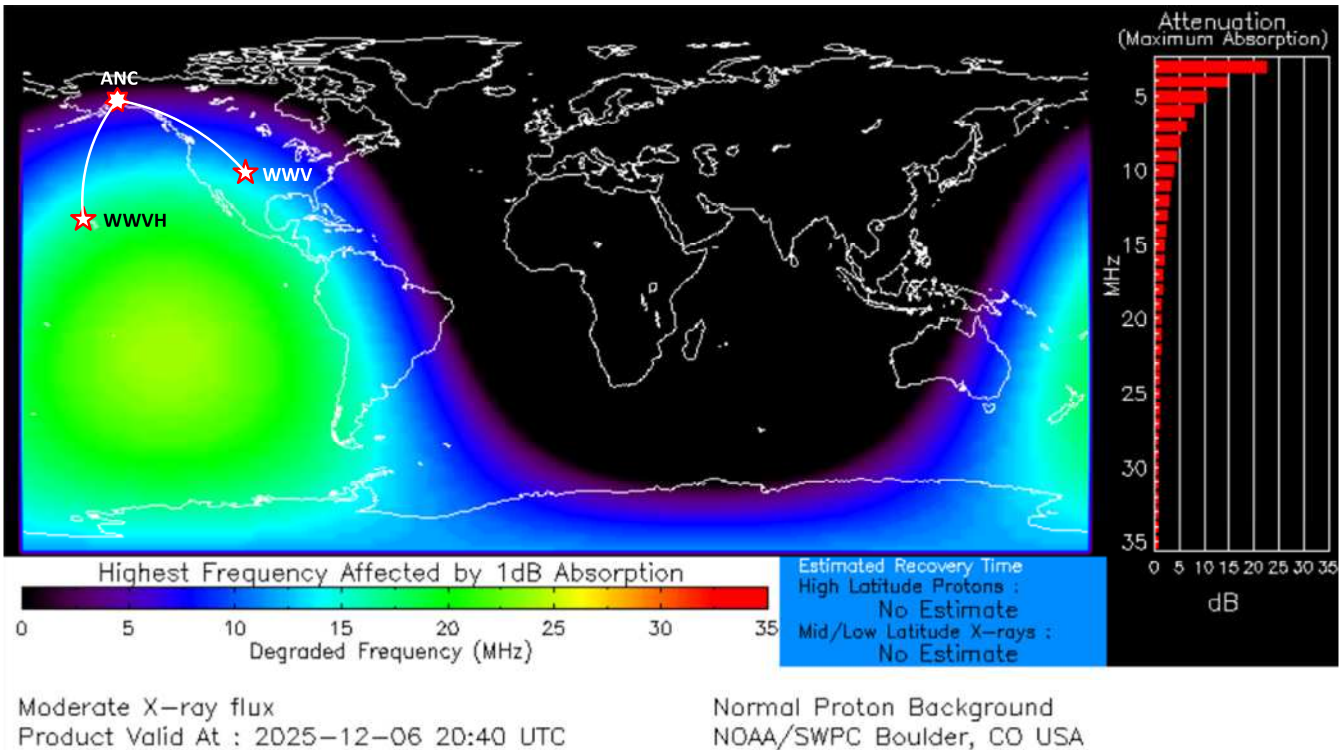

Figure 2 ~ D-Region Absorption Prediction (D-RAP) plot above for 2040 UTC. The three stations involved in this observation report are seen at upper-left. The predicted absorption at 15 MHz shown on the left histogram is less than 5 dB at 15 MHz but, whatever it actually was, it blacked out the path from WWVH. Underlying image source: https://www.swpc.noaa.gov/products/d-region-absorption-predictions-d-rap

Solar Radio Emissions

The Space Weather Prediction Center (SWPC) listed Type II slow radio sweeps and Type V fast radio sweeps in their Events report; see Appendix and {Events}. These emissions were received at the e-CALLISTO stations in Alaska {e-CALLISTO}; the spectral observations at the HAARP station were made while the Sun was only 4° above the horizon (figure 3). Other e-CALLISTO stations on Earth's dayside received the emissions as well.

The Type II slow radio sweep is the signature of a CME as it moves outward through the Sun's corona and encounters decreasing electron density and associated decreasing plasma frequency. The appearance of multiple overlaid Type II bursts could indicate the CME encountered varying density layers in a disturbed corona or different parts of the CME produced additional emissions as they moved through the corona.

The Type V radio burst consists of Type III fast radio bursts followed by a continuum emission lasting a few minutes. Type III bursts are the signature of near lightspeed electrons that are accelerated by a flare and beamed through the corona. The continuum that is associated with the Type III and gives it the Type V classification is not as well understood. Some explanations are low energy electrons traveling along different magnetic field lines, positional variations in the beaming process, or electron-cyclotron maser instability [Reid14].

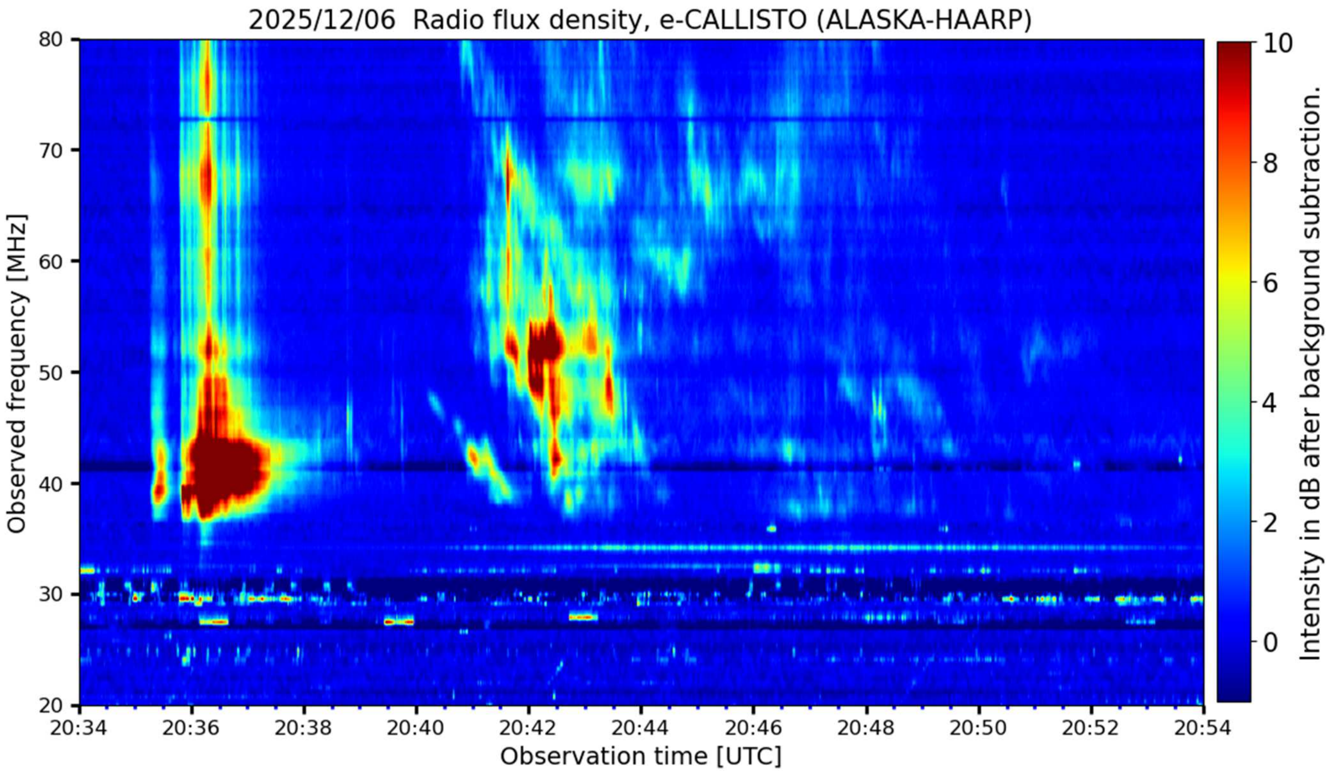

Figure 3 ~ Radio spectra received at HAARP Radio Observatory from 20 to 80 MHz. Note ionospheric cutoff around 35 MHz. The Type V from 2035 to 2039 with the characteristic continuum blob, and multiple Type II with harmonics and split bands from 2040 through 2052. The spectra below 35 MHz is from unknown terrestrial sources. Image courtesy of Christian Monstein from ALASKA-HAARP data at {e-CALLISTO).

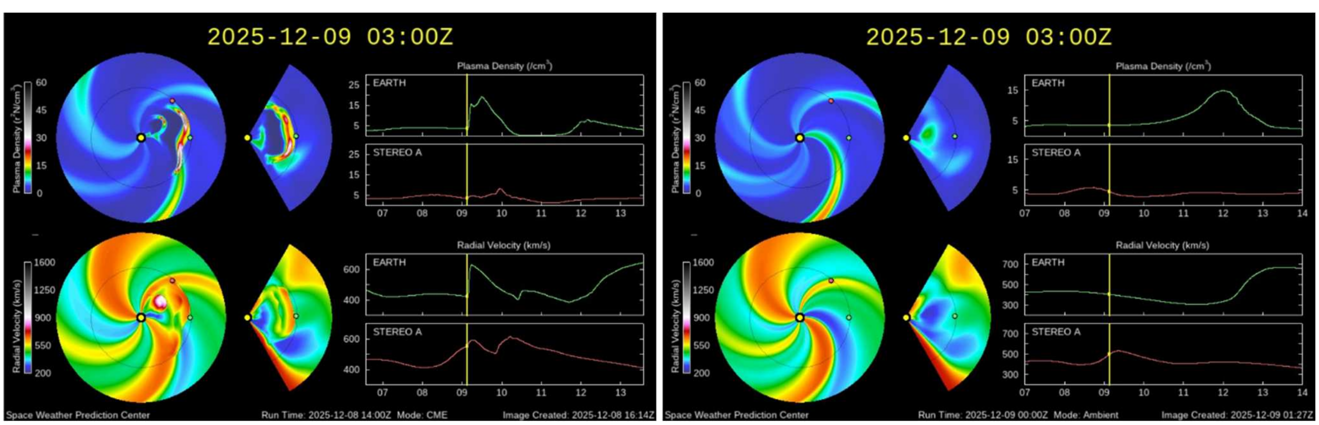

Figure 4 ~ WSA-ENLIL models of the CME prepared by Space Weather Prediction Center. The left image shows the prediction based on the initial review of satellite imagery; it shows significant effects at 0300 on 9 December (see yellow vertical cursor on the charts). However, the right image, which was based on a revised prediction run at 0000 on 9 December, shows no significant effects before or after 9 December. The circular plots are an overhead view of the Sun-Earth system and the pie-shaped plots are a view from Earth's orbital plane. The yellow Sun is at center and Earth is the small green circle right of center in both circular plots. The Sun is at left and Earth in the center of the pie-shaped plots. The upper plots are plasma density and the lower plots are solar wind radial velocity. Image source: https://www.swpc.noaa.gov/products/wsa-enlil-solar-wind-prediction

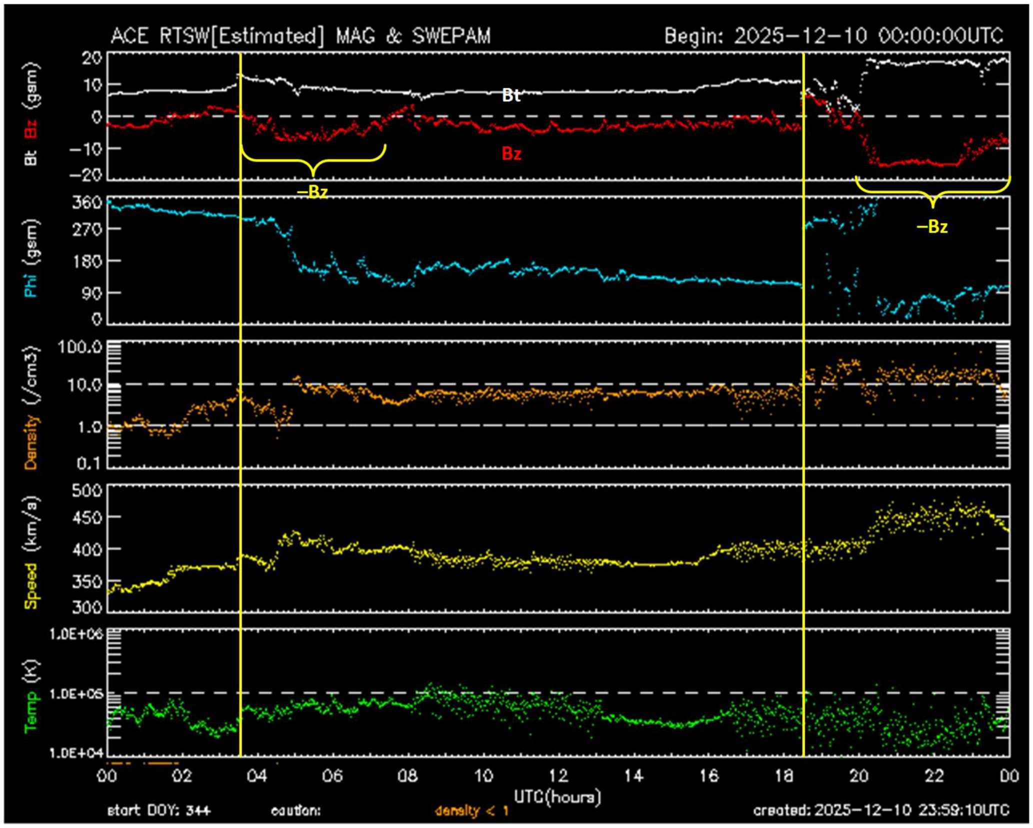

Figure 5 ~ Measurements at the ACE spacecraft 1.5 million km from Earth along the Earth-Sun line. A small magnetic field transient was detected at 0328 (left vertical yellow line) on 9 December followed by a negative transition of the Bz magnetic field component that lasted around 4 hours. Additional transient effects were detected around 1830 (right vertical yellow line) and also followed by negative Bz that persisted through 0300 the next day. SWPC reported the later activity as resulting from a *reverse shock* in the heliospheric current sheet.

Geomagnetic Effects

There were no instantaneous geomagnetic effects from the flare itself, but Space Weather Prediction Center initially predicted the CME would cause an increase in both the plasma density and solar wind speed at Earth on 9 December, potentially causing a magnetic disturbance. Later predictions showed no significant effects (figure 4). As it turned out, there were magnetic transients measured at the ACE spacecraft (figure 5),which preceded some unsettled activity measured by the SAM-III ground magnetometer at Anchorage on 10 December during the 0600 – 0900 and 2100 – 2400 synoptic periods (figure 6). The activity briefly increased to storm levels (K5) early the next day.

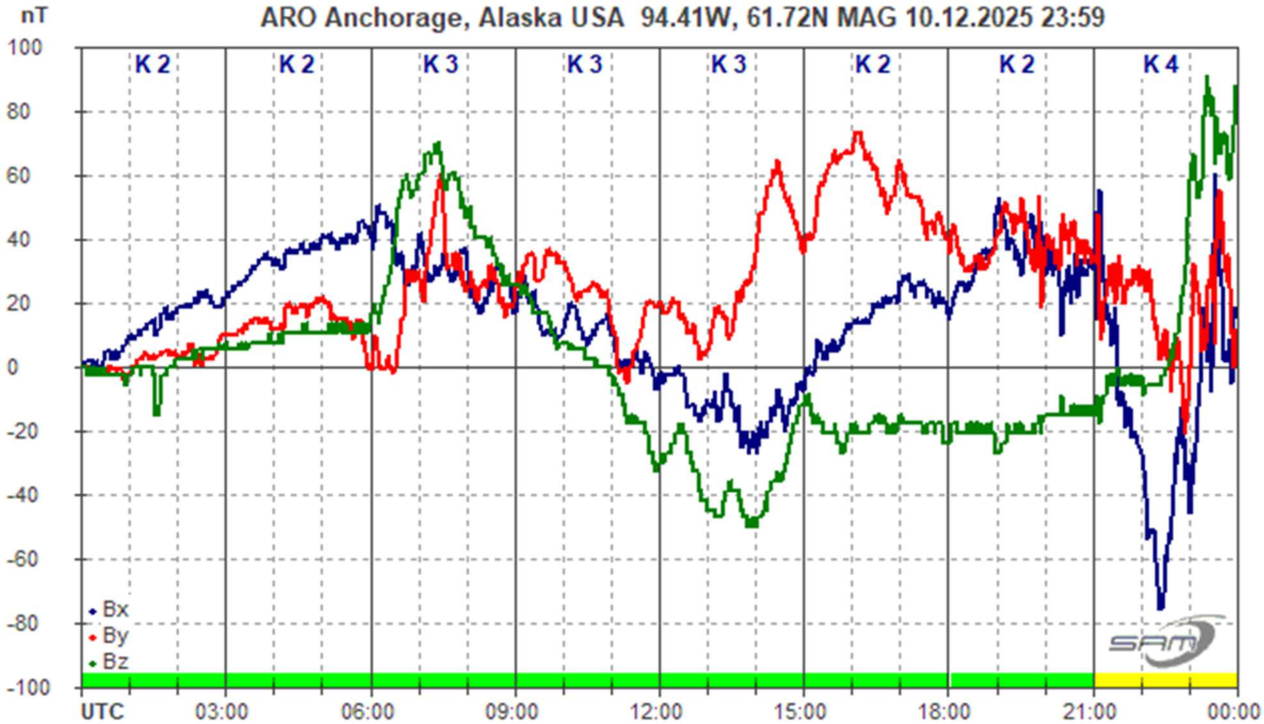

Figure 6 ~ SAM-III magnetogram for 10 December, four days after the flare and associated radio effects, showing relatively minor magnetic disturbances starting at 0600 and again at 2100. Both probably were related to the episodes of negative Bz seen in the ACE spacecraft magnetic field and solar wind data above and due to the CME. The activity shown at the end of day continued for three hours on 11 December with storm conditions (K5) reached at 0230 and followed almost immediately by quiet conditions. The magnetogram for 9 December (not shown) indicated a magnetically quiet day.

References

{e-CALLISTO} https://e-callisto.org/

{Events} ftp.swpc.noaa.gov/pub/indices/events/

{Reeve15a} Reeve, W. Sudden Frequency Deviations Caused by Solar Flares, Part I ~ Concepts, Available at: https://www.reeve.com/Documents/Articles%20Papers/Propagation%20Anomalies/Reeve_SuddenFreqDevConcepts_P1.pdf

{Reeve15b} Reeve, W. Sudden Frequency Deviations Caused by Solar Flares, Part II ! ~ Instrumentation and Observations , Available at: https://www.reeve.com/Documents/Articles%20Papers/Propagation%20Anomalies/Reeve_SuddenFreqDevMeas_P2.pdf

[Reid14] Reid, H.A.S., Ratcliffe, H., A Review of Solar Type III Radio Bursts, Research in Astronomy & Astrophysics, RAA 2014 Vol. 14 No. 7, 773–804 doi: 10.1088/1674–4527/14/7/003

Appendix

Space Weather Prediction Center Events Report, partial from {Events}

#Event	Begin	Max	End	Obs	Q	Type	Loc/Frq	Particulars		Reg#
2320 +	2029	2039	2049	G18	5	XRA	1-8A	M8.1	5.3E-02	4299

2340	2031	////	2055	HOL	3	DSF	N23W00	10	B.9A	4299
2320	2035	////	2039	PAL	C	RSP	025-180	V/3		
2320	2035	2036	2039	PAL	G	RBR	2695	1100		
2320	2035	2035	2039	PAL	G	RBR	410	12000		
2320	2035	2036	2037	PAL	G	RBR	1415	1700		
2320	2035	2036	2039	PAL	U	RBR	4995	900		
2320	2035	2036	2043	PAL	G	RBR	610	1100		
2320	2035	2036	2039	PAL	G	RBR	8800	580		
2320	2036	2037	2039	PAL	G	RBR	15400	310		
2320	2040	////	2056	PAL	C	RSP	025-180	II/3	1143	
2320 +	2048	2048	2050	PAL	G	RBR	245	660		

Document Information

Author: Whitham D. Reeveh

Revisions: 0.0 (Started, 06 Dec 2025)
0.1 (Edits, 09 Dec 2025)
0.2 (Added updated ACE data, 10 Dec 2025)
0.3 (Final edits for distribution, 11 Dec 2025)